Published in IET Communications
Received on 14th August 2013
Revised on 1st December 2013
Accepted on 19th December 2013
doi: 10.1049/iet-com.2013.0645

ISSN 1751-8628

Aggregate interference modelling and static resource allocation in closed and open access femtocells

Azam S. Hosseinzadeh-Salati, Masoumeh Nasiri-Kenari

Wireless Research Laboratory, Department of Electrical Engineering, Sharif University of Technology, Tehran, Iran
E-mail: Salaty@ee.sharif.edu

Abstract: Femtocell has appeared as a solution to increase both the coverage and the capacity of cellular networks. However, interference problem between the macrocell and the femtocell must be solved before any deployment. Since femtocells are deployed by home users in random locations, decentralised interference management schemes remain worth of investigation. In this study, the author deal with the problem of aggregate interference modelling and static resource allocation in orthogonal frequency division multiple access (OFDMA)-based two-tier femtocell networks for both closed and open access femtocells. It is assumed that for macrocell users (MUs), spectrum allocation is accomplished through fractional frequency reuse. The author's objective is to maximise the femtocell user's throughput while maintaining as low as its possible impact on the MUs' performance. Their proposed algorithm is decentralised, and based on some measurements, needs to be performed only when femtocell access point is plugged in. Simulation results show the accuracy of their model and the effectiveness of the proposed scheme compared to the previous methods.

1 Introduction

One of the main problems of emerging next generation wireless networks is the increase in the capacity demand. Previous studies show that the capacity of wireless networks can be highly increased by deploying smaller cell size [1]. However, this approach is not cost effective for macrocell BSs; leading to the introduction of femtocells. Femtocells are small, low power and inexpensive base stations designed to be mounted in an indoor area by the home user on a plug-and-play basis, and provide almost all of the cellular functionalities to the end users [2, 3]. One of the key advantages of this new technology is better coverage and improved quality of service (QoS) for high data rate services usually requested by indoor users. Moreover, battery life is increased because of the short distance of transmission. Further, the mobile operator benefits from the traffic switch over the wired backhaul and the reuse of resources, which improves the whole cellular network capacity.

Along with these benefits, femtocell networks face some technical challenges such as interference management, hand-off, synchronisation, self-organisation and security. Since femtocell access points (FAPs) operate in the licensed cellular band, the main problem in joint macrocell–femtocell deployments is the interference management [4]. Here, the interference management refers to all techniques aiming to decrease the effects of co-tier and cross-tier interferences such as resource allocation and access techniques. Femtocells may be deployed in closed or open access modes. A closed access FAP only serves specified home subscribers to ensure privacy and security. However, an open access FAP serves near MUs as well, in order to control the cross-tier interference at the cost of losing some of its resources and security [2, 5].

Next generation communication standards such as long term evolution (LTE) and WiMAX employ OFDMA to achieve higher data rates and enhanced spectral efficiency. In OFDMA, by allocating the frequency and time resources to users in an orthogonal manner, intracell interference is mitigated. Intercell interference is planned to be alleviated through fractional frequency reuse (FFR) [6–8]. In the conventional FFR known as soft frequency reuse (SFR), the whole channel bandwidth is divided into three sub-bands. Users in the outer region of adjacent sectors operate on different sub-bands as illustrated in Fig. 1, since they are more subjected to intercell interference. However, users in the inner region may operate on all sub-bands. For other kinds of FFR please see [9].

Several resource allocation techniques are proposed for two-tier femtocell networks. Since FAPs will be placed by end users in *ad hoc* locations and because of the present lack of coordination between the macrocell BS and the FAPs, a decentralised resource allocation deserves to receive more investigations. Further, any effective resource allocation scheme must satisfy the QoS requirements of all macrocell and femtocell users in addition to having low overhead and complexity. In [10–12], dynamic resource allocation schemes are proposed to achieve higher spectral efficiency compared with static approaches. However, these techniques are complicated and suffer from a large amount of overhead. Moreover, they require the FAP to have a frequent communication with the macrocell BS, or the ability of sensing the radio environment and recognising the interference signature accurately.

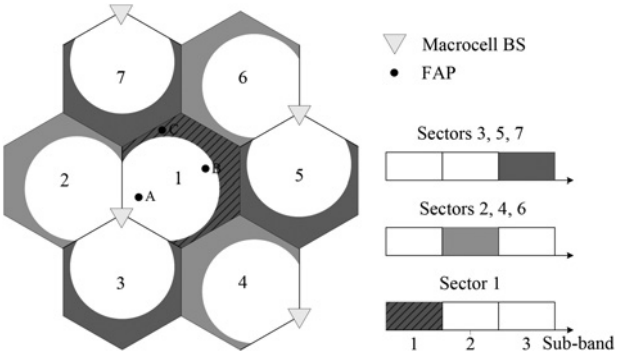

Fig. 1 *Sub-band allocations to MUs when SFR is used*

Currently, FFR is being considered as an effective interference management scheme for OFDMA-based two-tier femtocell networks [4]. The exhaustive comparison between different interference management schemes presented in [4] indicates that FFR-based static resource allocation schemes show high efficiency in interference management despite of their low complexities. In [13–15], static spectrum allocations of femtocells are investigated when FFR is used in the first tier. In these methods, femtocell simply uses the sub-bands that are not in use by neighbour MUs to manage the inter tier interference. In [16], FFR is exploited in the femto tier, as a solution to moderate femto-to-femto interference in a dense femtocell deployment. However, in order to manage inter tier interference which is the scope of this paper, Chowdhury *et al*. [16] uses a same approach as others, that is, simply allocating sub-bands that are not in use by neighbour MUs to femtocells. In [17], a static sub-band allocation method based on the pilot power of the macrocell BS is proposed for the downlink. Although these static methods are very simple, they do not lean on an analytic background and suffer from non-optimal performance.

In this paper, we study the problem of FFR-based static resource allocation in the uplink of two-tier OFDMA-based femtocell networks. To this end, we first model the uplink interference caused by MUs at the FAP for both closed and open access modes. Although the interference statistics have been investigated in [18] for a single cell scenario, here we consider a multi cell FFR-based scenario and model the interference for open access as well as closed access femtocells. Moreover, we take into consideration a more precise channel model and also derive the aggregate interference model from all neighbouring interfering sectors. We then propose a decentralised static resource allocation scheme according to the interference statistics, in which each FAP chooses its best sub-band in a distributed manner in order to reach the maximum throughput. In addition, the FAP's power is adjusted according to the maximum acceptable value of the outage probability at the FAP, while guaranteeing negligible effect on the throughput of the macro tier. Moreover in the open access mode, we determine the size of the FAP's serving area and the proportion of the femtocell bandwidth dedicated to a handed over MU jointly with the FAP's best sub-band to achieve the maximum throughput, while maintaining the performance of the handed over MU. Although this method requires somehow intensive calculations, the calculations need to be performed once in a while, that is, whenever the FAP is plugged in.

The rest of this paper is organised as follows. In Section 2, the system model is presented. In Section 3, the interference models for both closed and open access femtocells are provided. Moreover, the throughput and the outage probability for a femtocell user are calculated. In Section 4, the proposed resource allocation scheme is introduced, and in Section 5, analytical results are evaluated by simulations. Finally, the paper is concluded in Section 6.

2 System model

2.1 Macro tier

For the macro tier, we consider a reference sector (sector 1 which includes our FAP) and $K-1$ interfering neighbour sectors. Let each sector k be modelled with a circle of radius R_k and its inner region with a circle of radius R_k^{in} as illustrated in Fig. 2. We assume that SFR is employed in the macro tier of the network. Each sub-band is composed of N OFDMA resource blocks (RBs), that is, $3N$ RBs on the whole band. The MUs' positions are assumed to be i.i.d. random variables, uniformly distributed within the sector. For simplicity and without loss of generality, we assume that all MUs have the same target rates with one RB allocated to each user. As a result, there are a maximum of $3N$ active MUs roaming inside each sector, namely, $2N$ inner users as well as N outer users. That is, the ratio of R_k to R_k^{in} is selected such that the area of the inner region will be twice the area of the outer region, that is, $R_k/R_k^{\text{in}} = \sqrt{3/2}$. Here, we assume that the FAP does not have the ability of sensing the radio spectrum, and thus we do our analyses based on the worst case, that is, we assume that all RBs are occupied at all times. Then, we sort MUs according to their allocated RBs.

2.2 Femto tier

We consider a femtocell in the reference sector with one active user which is completely synchronised with its serving BS. Let D_k denote the distance between this FAP and the BS of sector k, and γ_k correspond to the angle of the FAP with reference to the centre line of sector k (Fig. 2). The FAP chooses its best operating sub-band by having all D_ks and γ_ks. Then, a number of RBs of its specified sub-band are randomly chosen, according to its backhaul bandwidth. For an open access FAP, all interfering MUs in the R_f vicinity of the FAP that operate on the same RB as the femtocell, will be handed over to the

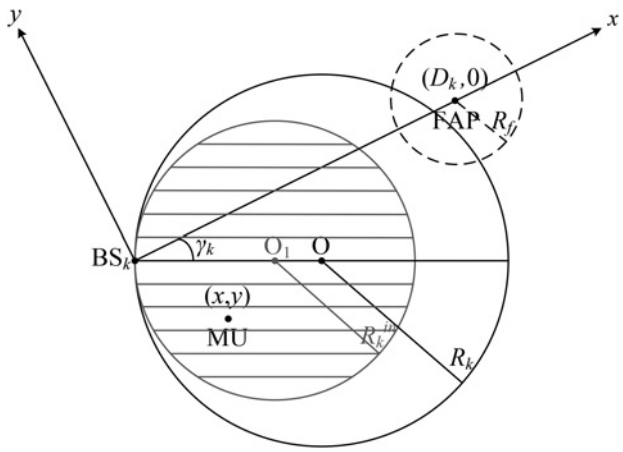

Fig. 2 *Inner region (hatched) and outer region (solid) of the sector k and the FAP location*

doi: 10.1049/iet-com.2013.0645

FAP, that is, a serving region of radius R_f is assumed around the FAP (the dashed circle in Fig. 2). Then, the FAP allocates a proportion λ_h of its bandwidth to each handed over MU. Here, we ignore femto-to-femto interference for simplicity and to converge on a decentralised static approach.

2.3 Channel model

We take into account path loss effects for the channel model as well as fading and shadowing, that is, the channel gain equals to

$$g_{\mathrm{Tx}\to\mathrm{Rx}} = d^{-\alpha}Hw \tag{1}$$

where α is the path loss exponent, d is the distance between a user (Tx) and its desired BS (Rx), H is the channel gain for the composite shadowing and fading effects and w is the wall penetration loss included in the channel gain when the transmission is done through the wall. Here we consider log-normal shadowing and Rayleigh fading. Therefore, the probability density function (PDF) of the composite shadowing and fading effects of the channel, that is, H, is approximated by a new log-normal distribution [19]

$$f_H(h) \simeq \frac{10}{\ln(10)\sqrt{2\pi}\sigma h}\exp\left\{-\frac{\left(10\log_{10}(h)-\mu\right)^2}{2\sigma^2}\right\} \tag{2}$$

where $\mu = \mu_{\mathrm{sh}} - 2.50675$ and $\sigma^2 = \sigma_{\mathrm{sh}}^2 + 31.0215$, with μ_{sh} and σ_{sh}^2 standing for the mean and variance of the log-normal shadowing distribution.

2.4 Power control

Uplink power control is assumed to be performed in the macro tier of the cellular network such that the received powers at the macrocell BSs are equal to P_m. This implies that the MU j of the sector k causes interference power of $P_m I_{jk}$ at the FAP, where I_{jk} is its interference factor at the FAP. Moreover, in the femto tier, the power control procedure is set to reach the target power P_f at the FAP unless we consider a scenario in which this target power is selected according to the location of the FAP to achieve a better interference management. We will discuss more on this topic in Section 4.

3 Interference modelling and performance analysis

In this section, we first model the interference factor caused by a MU at the FAP, for closed and open access femtocells in parts A and B. Next, in part C, we model the aggregate interference from all neighbouring sectors. Finally, in part D, the throughput and the outage probability for the home user are calculated according to the aggregate interference statistics.

3.1 Closed access

In [20], we have defined N i.i.d. interference factors, I_{jk}, $j = (s-1)N+1$, $(s-1)N+2$, …, sN, with s denoting the index of the specified sub-band. To be precise, I_{jk} is the ratio of the channel gain between user j of sector k and the FAP to the channel gain between this user and its relevant macrocell BS. Then, separate formulations for the cumulative distribution functions (CDFs) of the interference factors because of an inner and an outer MU have been derived. In this part, we rewrite those formulations in compact forms that are more convenient for the open access mode calculations.

To investigate the interference effect of inner region MUs of sector k on the FAP, here we define a coordinate system with the base station position specified as its origin. Then, the x-axis is determined such that it comprises the FAP position, that is, $(D_k,0)$ stands for the coordinates of the FAP (Fig. 2). Moreover, in this figure, (x,y) represents the coordinates of the MU j of sector k. Thus, the CDF of the interference factor of this MU (I_{jk}) at the FAP when considering just path loss for the channel can be written as

$$\begin{aligned}\bar{F}_{\mathrm{k,C}}^{\mathrm{in}}(l) &= \mathbb{P}(I_{jk}\le l) = \mathbb{P}\left(\frac{g_{\mathrm{MU}\to\mathrm{FAP}}}{g_{\mathrm{MU}\to\mathrm{BS}}}\le l\right)\\ &= \mathbb{P}\left(\frac{d_{\mathrm{MU}\to\mathrm{FAP}}^{-\alpha}}{d_{\mathrm{MU}\to\mathrm{BS}}^{-\alpha}}\le l\right) = \mathbb{P}\left(\frac{(D_k^2+x^2+y^2-2D_kx)^{-(\alpha/2)}}{(x^2+y^2)^{-(\alpha/2)}}\right.\\ &\left.\le l\,\middle|\,(x,y)\in\text{inner region of sector } k\right)\\ &= \mathbb{P}\big((1-l^{(2/\alpha)})x^2+(1-l^{(2/\alpha)})y^2+2D_kxl^{(2/\alpha)}\\ &\quad -D_k^2l^{(2/\alpha)}\le 0|(x,y)\in\text{inner region of sector } k\big)\end{aligned} \tag{3}$$

where g is the path loss channel defined as $d^{-\alpha}$ with d denoting the distance between the MU and its desired receiver (FAP or BS) and α indicating the path loss exponent. Moreover, D_k denotes the distance between the FAP and the BS of sector k. Subscript 'C' indicates the closed access mode and superscript 'in' points to the inner region calculations. Now, we specify the regions by different sets. Let set M_k^{in} denote the inner region of the sector k, and M_k for the whole sector. We also define the region specified by $(1-l^{(2/\alpha)})x^2+(1-l^{(2/\alpha)})y^2+2D_kxl^{(2/\alpha)}-D_k^2l^{(2/\alpha)}\le 0$ in (3) as $I_k(l)$. Consequently, $\bar{F}_{\mathrm{k,C}}^{\mathrm{in}}(l)$ can be expressed as

$$\begin{aligned}\bar{F}_{\mathrm{k,C}}^{\mathrm{in}}(l) &= \mathbb{P}(I_{jk}\le l) = \mathbb{P}P\big((x,y)\in I_k(l)|(x,y)\in M_k^{\mathrm{in}}\big)\\ &= \frac{S\big(M_k^{\mathrm{in}}\cap I_k(l)\big)}{S(M_k^{\mathrm{in}})}\end{aligned} \tag{4}$$

where $S(.)$ is a function that calculates the area of the region specified as its argument. Note that unlike other regions, the shape and size of $I_k(l)$ changes with l. That is, when $l<1$, the region is in fact the inner region of a circle with radius $r = D_k l^{1/\alpha}/|1-l^{2/\alpha}|$ centred at O_2 $(x_c,0)$ where $x_c = -D_k l^{2/\alpha}/(1-l^{2/\alpha})$ (Fig. 3*a*), and when $l=1$, it is the region specified with $x\le D_k/2$. However, for $l>1$, $I_k(l)$ corresponds to the outer region of a circle with centre O_2 at $(x_c,0)$ and radius r. Therefore, in this case ($l>1$), we write our formulas based on $I_k^{\mathrm{c}}(l)$, that is, the region inside the predefined circle, instead of $I_k(l)$ (Fig. 3*b*). In these figures, the hatched region specifies M_k^{in} and the dotted region specifies $I_k(l)$. As a result, $\bar{F}_{\mathrm{k,C}}^{\mathrm{in}}(l)$ is obtained as

$$\bar{F}_{\mathrm{k,C}}^{\mathrm{in}}(l) = \begin{cases}\dfrac{S(M_k^{\mathrm{in}}\cap I_k(l))}{S(M_k^{\mathrm{in}})} & l\le 1\\ 1-\dfrac{S(M_k^{\mathrm{in}}\cap I_k^{\mathrm{c}}(l))}{S(M_k^{\mathrm{in}})} & l>1\end{cases} \tag{5}$$

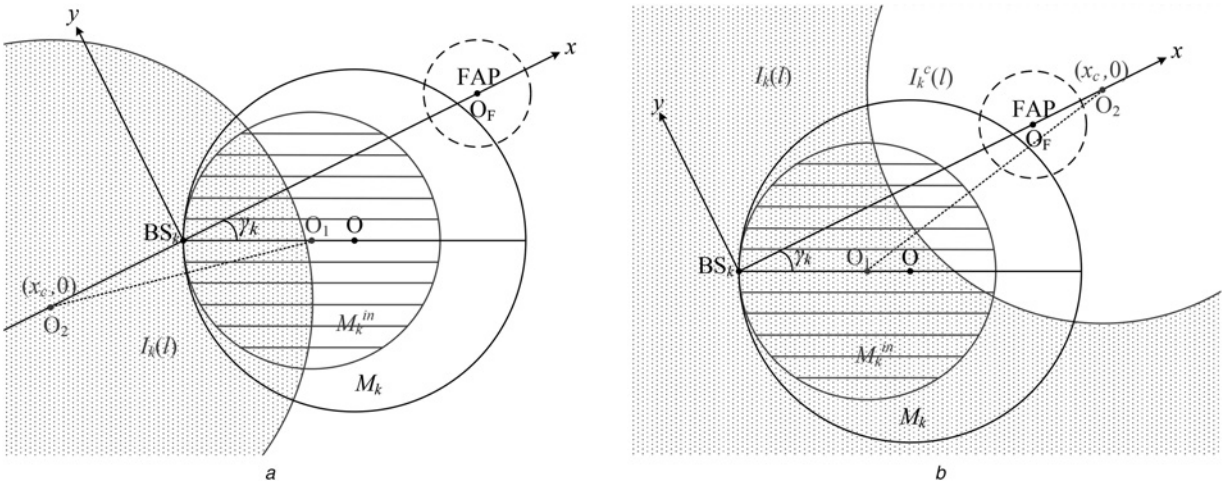

Fig. 3 *$I_k(l)$ and its intersection with M_k^{in} for typical values of l*
a $l<1$
b $l>1$

From (5), the CDF can be easily computed by calculating the intersection area of circles M_k^{in} and $I_k(l)$ (or $I_k^{\text{c}}(l)$) with R_k^{in} and r as the circles' radii and $D_{O_1O_2} = \sqrt{x_c^2 + R_k^{\text{in}2} - 2x_c R_k^{\text{in}} cos(\gamma_k)}$ as the distance between two centres (please see the Appendix for more details). For an outer region interfering MU, the CDF of the interference factor (with superscript 'out') is calculated similarly as

$$\bar{F}_{\text{k,C}}^{\text{out}}(l) = \begin{cases} \dfrac{S(M_k \cap I_k(l)) - S(M_k^{\text{in}} \cap I_k(l))}{S(M_k) - S(M_k^{\text{in}})} & l \le 1 \\ 1 - \dfrac{S(M_k \cap I_k^{\text{c}}(l)) - S(M_k^{\text{in}} \cap I_k^{\text{c}}(l))}{S(M_k) - S(M_k^{\text{in}})} & l > 1 \end{cases} \tag{6}$$

As mentioned in the previous section, the composite shadowing and fading effects of the channel have a near log-normal distribution, that is, as $10^{-Z/10}$, where Z is a Gaussian random variable. Thus, the conditional CDF of the interference factor with the more precise channel model of (1) will be

$$\begin{aligned} &F_{\text{k,C}}^{\text{in}}\left(l|Z_1 = z_1, Z_2 = z_2\right) \\ &\quad = \mathbb{P}\left(\frac{(D_k^2 + x^2 + y^2 - 2D_k x)^{-(\alpha/2)} 10^{-(Z_1/10)} w}{(x^2 + y^2)^{-(\alpha/2)} 10^{-(Z_2/10)}}\right. \\ &\qquad \left. \le l \middle| (x,y) \in M_k^{\text{in}}, Z_1 = z_1, Z_2 = z_2\right) \\ &\quad = \bar{F}_{\text{k,C}}^{\text{in}}\left(10^{((Z_1 - Z_2)/10)} w^{-1} l | Z_1 = z_1, Z_2 = z_2\right) \end{aligned} \tag{7}$$

which reduces to the predefined CDF in (3). Note that since the locations of different MUs are i.i.d. random variables, their channel gains to the FAP and to the macrocell BS are also independent and as a result, random variables I_{jk}, $j = (s-1)N+1, (s-1)N+2, \ldots, sN$, are i.i.d. for each k. In this equation, Z_1 and Z_2 are the Gaussian random variables possibly with different means and variances that are relevant to the composite shadowing and fading effects of the user channels to the FAP and to the BS, respectively. Now, $H = 10^{((Z_1 - Z_2)/10)}$ has a log-normal distribution with mean $\mu = \mu_1 - \mu_2$ and variance $\sigma^2 = \sigma_1^2 + \sigma_2^2$ with the PDF $f_H(h)$ defined in (2). Accordingly, $F_{\text{k,C}}^{\text{in}}(l)$ is expressed as

$$F_{\text{k,C}}^{\text{in}}(l) = \int_0^\infty f_H(h) \bar{F}_{\text{k,C}}^{\text{in}}(Hw^{-1} l | H = h) \text{d}h \tag{8}$$

and the same is derived for the interference factor of outer MUs as

$$F_{\text{k,C}}^{\text{out}}(l) = \int_0^\infty f_H(h) \bar{F}_{\text{k,C}}^{\text{out}}(Hw^{-1} l | H = h) \text{d}h \tag{9}$$

3.2 Open access

In the open access mode, the MUs served by the FAP do not cause interference, and thus is not considered in interference calculations. That is, the interfering MUs have a uniform distribution around the inner region except on the serving region of the FAP, that is, $M_k^{\text{in}} - F$ where set F indicates the serving region of the FAP. Thus, the CDF of the interference factor because of an inner MU of sector k at an open access FAP is governed by

$$\begin{aligned} \bar{F}_{k,\text{O}}^{\text{in}}(l) &= \mathbb{P}(I_{jk} \le l) \\ &= \mathbb{P}\left((x,y) \in I_k(l) | (x,y) \in M_k^{\text{in}} - F\right) \\ &= \frac{S(M_k^{\text{in}} \cap I_k(l)) - S(M_k^{\text{in}} \cap I_k(l) \cap F)}{S(M_k^{\text{in}}) - S(M_k^{\text{in}} \cap F)} \end{aligned} \tag{10}$$

where subscript 'O' denotes the open access mode. Since in this mode, the FAP only serves the close interfering MUs (which are reasonably more closer to the FAP than their serving BSs), its serving area would not have any overlap with $I_k(l)$ for $l \le 1$, that is, $I_k(l) \cap F = \emptyset$ for $l \le 1$. So, the

doi: 10.1049/iet-com.2013.0645

CDF of the interference factor equals to

$$\bar{F}^{\text{in}}_{k,\text{O}}(l) = \begin{cases} \dfrac{S(M^{\text{in}}_k \cap I_k(l))}{S(M^{\text{in}}_k) - S(M^{\text{in}}_k \cap F)} & l \le 1 \\ 1 - \dfrac{S(M^{\text{in}}_k \cap I^c_k(l)) - S(M^{\text{in}}_k \cap I^c_k(l) \cap F)}{S(M^{\text{in}}_k) - S(M^{\text{in}}_k \cap F)} & l > 1 \end{cases} \tag{11}$$

and this function for an outer region interfering MU will easily be (see (12))

The regions in these equations are simply a circle or the intersection of two or three circles. As for the case of two circles, the intersection area of three circles can be determined by having the circles' radii and the distances between each two circle centres [21]. However, these calculations are not easy, and therefore we have made some approximations for the case of three circles considered here (see the Appendix).

To derive the results for the more precise channel model, we should take the same procedures as in the closed access mode, that is, (8) and (9) will be simply employed for the CDF of interference factor because of inner and outer MUs, respectively.

3.3 Aggregate interference from all sectors

Total interference factor at the FAP on each RB is because of K active MUs with the same allocated RB (say RB j), each in different sectors. We observed that the CDF of each I_{jk} depends primarily on whether the MU j is an inner or an outer user of sector k or equally on the sub-band s that the RB j belongs to. Thus, the CDF of the total interference factor is written as

$$G^s(l) = \mathbb{P}\left(\sum_k I_{jk} \le l\right) = \int_{\sum_k l_k \le l} \cdots \int f^s_I(l_1, \ldots, l_K)\mathrm{d}l_1 \ldots \mathrm{d}l_K \tag{13}$$

where $f^s_I(l_1, \ldots, l_K)$, is the joint PDF of I_{jk}, $k = 1, \ldots, K$, and depends mainly on the sub-band comprising the RB j. We should note that the spectrum allocation policy in the macro tier may result in the dependency between the locations of the users with the same RBs which results in the dependency between the distances of these users to the FAP. However, this would not necessarily result in the dependency of their interference factors, since this is just one of the parameters that influences on the interference factor. To be more precise, independent distances of these users to their relevant BS, and independent shadowing and fading effects of their channels to the FAP and to their relevant BS considerably weaken the dependency of their interference factors, because of the notable effect of these parameters on the value of the interference factor. So, we assume that the interference components because of these K MUs, that is, I_{jk}, $k = 1, \ldots, K$ are independent but not identically distributed random variables, and thus their joint PDF is the product of their PDFs or equivalently, the PDF of the total interference factor is the K-fold convolution of the PDFs. When frequency resources for MUs are allocated through an FFR pattern, the joint PDF is easily computed as

$$f^s_I(l_1, \ldots, l_K) = \prod_{k \in O_s} f^{\text{out}}_k(l_k) \prod_{k \notin O_s} f^{\text{in}}_k(l_k) \tag{14}$$

where O_s is the set of sectors that specify sub-band s to their outer users, and $f_k(l_k) = \partial F_k(l_k)/\partial l_k$ (with superscript 'in' or 'out') is the PDF of the interference factor because of a MU of sector k at the FAP. It is obvious from (13) that the aggregate interferences observed at different RBs of the same sub-band are i.i.d. random variables. These results are applicable for both closed and open access modes.

3.4 Throughput and outage calculations

Suppose C be the target rate for the home user served by the FAP in bps/Hz. With adaptive modulation and coding, the value of C depends on the channel condition and varies with the value of signal-to-interference-plus-noise ratio (SINR). Suppose that there are N_C possible target rates on the whole, that is, $\{C_i\}_{i=1}^{N_C}$. Since each MU causes interference to the femtocell user on its allocated RB, namely, RB j, the femtocell user's throughput, when using sub-band s, is given by

$$\begin{aligned} T^s_{\text{f}} &= \frac{W}{N} \sum_{j=(s-1)N+1}^{sN} T_j = \frac{W}{N} \sum_{j=(s-1)N+1}^{sN} \left[\sum_{i=1}^{N_C-1} C_i \mathbb{P}(\Gamma_i \le \text{SINR}_j < \Gamma_{i+1}) + C_{N_C}\mathbb{P}(\text{SINR}_j \ge \Gamma_{N_C})\right] \\ &= \frac{W}{N} \sum_{j=(s-1)N+1}^{sN} \left[\sum_{i=1}^{N_C-1} C_i \mathbb{P}\left(\Gamma_i \le \frac{P_{\text{f}}}{P_{\text{m}}\sum_k I_{jk} + \sigma^2} < \Gamma_{i+1}\right) + C_{N_C}\mathbb{P}\left(\frac{P_{\text{f}}}{P_{\text{m}}\sum_k I_{jk} + \sigma^2} \ge \Gamma_{N_C}\right)\right] \\ &= W\left[\sum_{i=1}^{N_C-1} C_i\left[G^s\left(\frac{P_{\text{f}}}{P_{\text{m}}\Gamma_i} - \frac{\sigma^2}{P_{\text{m}}}\right) - G^s\left(\frac{P_{\text{f}}}{P_{\text{m}}\Gamma_{i+1}} - \frac{\sigma^2}{P_{\text{m}}}\right)\right] + C_{N_C} G^s\left(\frac{P_{\text{f}}}{P_{\text{m}}\Gamma_{N_C}} - \frac{\sigma^2}{P_{\text{m}}}\right)\right] \end{aligned} \tag{15}$$

Note that the last equality is governed by the i.i.d. property of the term $\sum_k I_{jk}$ for different values of j of the same sub-band. In this equation, T_j is the throughput because of the RB j which is a summation over all possible rates, W is the allocated bandwidth of the femtocell, Γ_i is the target SINR

$$\bar{F}^{\text{out}}_{k,\text{O}}(l) = \begin{cases} \dfrac{S(M_k \cap I_k(l)) - S(M^{in}_k \cap I_k(l))}{S(M_k) - S(M_k \cap F) - S(M^{\text{in}}_k) + S(M^{\text{in}}_k \cap F)} & l \le 1 \\ 1 - \dfrac{S(M_k \cap I^{\text{c}}_k(l)) - S(M_k \cap I^{\text{c}}_k(l) \cap F) - S(M^{\text{in}}_k \cap I^{\text{c}}_k(l)) + S(M^{\text{in}}_k \cap I^{\text{c}}_k(l) \cap F)}{S(M_k) - S(M_k \cap F) - S(M^{\text{in}}_k) + S(M^{\text{in}}_k \cap F)} & l > 1 \end{cases} \tag{12}$$

according to the desired target rate C_i, P_m (P_f) is the macrocell (femtocell) user's received power at its serving BS (FAP) defined in Section 2, σ^2 is the noise power, and $G^s(.)$ is the CDF of the total interference derived in (13). Note that the number of allocated RBs to different MUs need not to be equal as we regard each RB, instead of each MU, as an interferer. Then, the outage probability is given by

$$\mathbb{P}^s_{\text{out}} = \mathbb{P}(\text{SINR} < \Gamma_1) = 1 - G^s\left(\frac{P_f}{P_m\Gamma_1} - \frac{\sigma^2}{P_m}\right) \quad (16)$$

We should note that for an open access FAP, W is partitioned to W_f for the femtocell user and W_h for all handed over MUs and thus, the throughput of the home user and handed over MUs will be $T^s_f = W_f \sum_j T_j/N$ and $T^s_h = W_h \sum_j T_j/N$, respectively. It is easy to formulate $W_h = N_h\lambda_h W$, where N_h is the number of handed over MUs, and λ_h is the proportion of the femtocell bandwidth dedicated to a handed over MU.

4 Proposed resource allocation scheme

With the aim of achieving the maximum throughput for the home user while having negligible impact on the macro tier, here we study the problem of the static resource allocation. According to (15), the throughput of a femtocell user depends primarily on the following parameters; the sub-band s on which it operates, the target power P_f and for an open access FAP, the serving region radius R_f, which effects on both W_f and $G^s(.)$, and λ_h, which effects on W_f.

In the following, we first deal with the problem of finding the target power in the power control procedure in part A. In part B, we then introduce our proposed sub-band allocation scheme for a closed access FAP. In part C, we consider the problem of jointly selecting the optimum sub-band, the radius of the serving region, and the proportion of the femtocell bandwidth dedicated to a handed over MU for an open access FAP.

4.1 Power allocation

An uplink power control is assumed to be applied in both two tiers of the network in a way to reach a target power at the relevant receiver. The power control procedure used in the macro tier results in unequal performance for near BS and edge femtocells. To solve this problem, in the femto tier, we propose the target power to be variable and dependent on the location of the FAP. Those FAPs located near the edge of the sector experience more interference from MUs, leading to large outage probabilities. On the other hand, a far femtocell has insignificant impact on the macro BS, and thus, its transmissions can be done with higher target power. As a result we consider a minimum and a maximum value for the target power of a femtocell, to ensure effective interference management in both FAP and macrocell BS.

Let $I = \sum_k I_{jk}$ be the total interference factor observed at the FAP, where j is an arbitrary RB of the operating sub-band of the femtocell (note that the aggregate interferences observed at different RBs of the same sub-band are i.i.d. random variables). Considering (16), we select the minimum target power as

$$P^{\min}_f = P_m\Gamma_1\left(\bar{I} + \frac{\sigma^2}{P_m}\right) \quad (17)$$

where $\bar{I}$ is the minimum value of I that ensures $P_{\text{out}} \le P^{\max}_{\text{out}}$ on the specified optimum sub-band.

On the other hand, we set $P^{\max}_f$ such that the femtocell user's interference power at the macrocell BS be at the range of the noise power. Thus, the femto tier interference is guaranteed to be negligible with respect to the dominant interference power from MUs of neighbouring sectors. For example, if we simply consider a path loss channel between the femtocell user and the macrocell BS, the interference power induced by the femtocell user at the macrocell BS will approximately be equal to $P_f D_1^{-\alpha}$, and consequently the maximum target power will be $\sigma^2 D_1^{\alpha}$.

4.2 Sub-band allocation for a closed access FAP

According to (15), the home user's throughput depends primarily on the FAP's operating sub-band for a closed access FAP. Thus, here we introduce an integer optimisation problem with a few possible values for the variable s (three possible values of 1, 2, 3 when SFR is used in the macro tier) that aims to maximise T^s_f. That is

$$\max_s T^s_f = \max_s W \times \left[\sum_{i=1}^{N_C-1} C_i\left[G^s\left(\frac{P_f}{P_m\Gamma_i} - \frac{\sigma^2}{P_m}\right) - G^s\left(\frac{P_f}{P_m\Gamma_{i+1}} - \frac{\sigma^2}{P_m}\right)\right] + C_{N_C}G^s\left(\frac{P_f}{P_m\Gamma_{N_C}} - \frac{\sigma^2}{P_m}\right)\right] \quad (18)$$

In the scheme proposed, P_f has to be known in the process of optimum sub-band allocation, and conversely, the optimum sub-band has to be known in order to find $\bar{I}$, and consequently, P_f. So, we select P_f and the sub-band iteratively until a convergence is achieved, that is, when P_f reaches $P^{\max}_f$, or the specified sub-band is unchanged in two successive iterations.

4.3 Joint resource allocation for an open access FAP

For an open access FAP, the home user's throughput depends on two other parameters R_f and λ_h. However, the optimum values for R_f, and λ_h are not easy to find as the exhaustive search has to be done in a real value domain. Thus, we propose a sub-optimum solution, in which we consider some possible reasonable discrete values for R_f and λ_h. That is, we select the best operating sub-band, and the values for R_f and λ_h among the possible values such that the maximum possible throughput for the femtocell is achieved, constrained on preserving at least the prior throughput of the handed over MU. Thus, we must solve the following discrete optimisation problem with three variables which each obtains a few number of possible values

$$\max_{s,R_f,\lambda_h} T^s_f = \max_{s,R_f,\lambda_h} W_f \times \left[\sum_{i=1}^{N_C-1} C_i\left[G^s\left(\frac{P_f}{P_m\Gamma_i} - \frac{\sigma^2}{P_m}\right) - G^s\left(\frac{P_f}{P_m\Gamma_{i+1}} - \frac{\sigma^2}{P_m}\right)\right] + C_{N_C}G^s\left(\frac{P_f}{P_m\Gamma_{N_C}} - \frac{\sigma^2}{P_m}\right)\right] \quad (19)$$

doi: 10.1049/iet-com.2013.0645

with a constraint on the throughput of the handed over MU

$$T_{\mathrm{h}}^{s}=\lambda_{\mathrm{h}}W\left[\sum_{i=1}^{N_C-1}C_i\left[G^{s}\left(\frac{P_{\mathrm{f}}}{P_{\mathrm{m}}\Gamma_i}-\frac{\sigma^2}{P_{\mathrm{m}}}\right)-G^{s}\left(\frac{P_{\mathrm{f}}}{P_{\mathrm{m}}\Gamma_{i+1}}-\frac{\sigma^2}{P_{\mathrm{m}}}\right)\right]+C_{N_C}G^{s}\left(\frac{P_{\mathrm{f}}}{P_{\mathrm{m}}\Gamma_{N_C}}-\frac{\sigma^2}{P_{\mathrm{m}}}\right)\right]\geq T_{\mathrm{m}}^{s} \quad (20)$$

where T_{m}^{s} is the throughput of the MU before the handover, and T_{h}^{s} is its throughput after the handover.

As in the closed access case, P_{f} is selected iteratively with other resources until a convergence is achieved.

Note that the above calculations must be done just the once the FAP is plugged in. Nevertheless, since the dominant computational complexity of our scheme is because of the K-fold convolution used to find the PDF of the total interference factor, our resource allocation scheme has a computational complexity of $O(n\log(n))$, where n is the length of each PDF vector.

5 Simulation results

We evaluate the performance of our proposed scheme based on both the analytical derivations and simulations. Here, we consider a total of seven equal size sectors for our analyses. By simulation, we evaluate the network throughput in the reference sector while the other sectors contribute as making interference to the reference sector. We perform our analysis for three femtocells located in different regions of the sector (Fig. 1), assuming that the femtocell user transmits on all RBs of the allocated sub-band. We run our simulations for 10 000 different arrangements of MUs. The values of our system parameters are given in Table 1. The SINR targets according to different rates are chosen based on the modulation and coding sets, taken from [22].

First, we study the characteristics of $G^{s}(l)$ for the FAP A as an example, which is located near the macrocell BS in the inner region of the sector, in both closed and open access modes with $R_{\mathrm{f}}=20$ m. We can see that the sub-band 1 that is used by outer MUs, is obviously the best one (Fig. 4). In the open access case, $G^{s}(l)$ is slightly improved for sub-bands 2 and 3 but it remains unchanged for sub-band 1 since there are no MUs operating on sub-band 1 in the R_{f}-vicinity of the FAP.

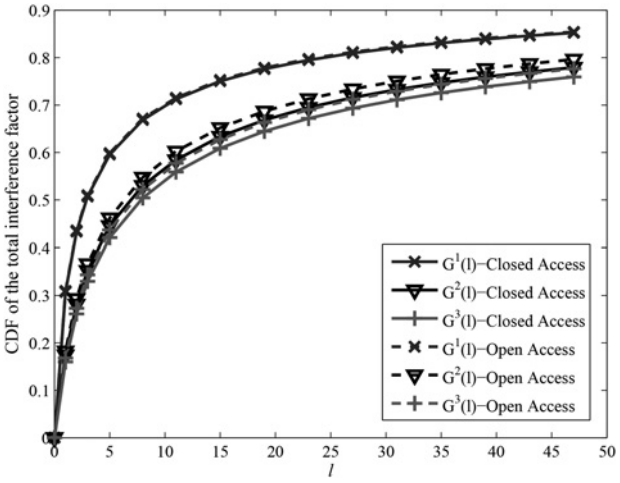

Fig. 4 *CDF of the total interference factor at the FAP A*

Next, we evaluate the CDF of the interference factor as an example at the FAP C which is located in the outer region of the sector in the closed access mode, and compare the simulation results with the analytical ones. Fig. 5 shows the accuracy of our model especially in determining the best sub-band.

We also evaluate the throughput of the home user of the FAP B in different sub-bands against the received SNR at the FAP (Fig. 6*a*). For this FAP, sub-bands 2 and 3 have almost similar performance according to the approximate symmetry in its position, and here, we only illustrate the results for the sub-bands 1 and 3 for clarity of the plots. Fig. 6*b* shows the home user outage probability on each sub-band in closed and open access modes. In the open access mode, we have set $R_{\mathrm{f}}=30$ m and $\lambda_{\mathrm{h}}=1/30$. We can see that the sub-band 3 (and 2) show considerable performance in both the throughput and the outage probability compared to the sub-band 1, which is proposed to be used by this femtocell in [13]. Although our analytical results have a little gap with the simulations (because of the approximations made in the specified model), they lead to

Table 1 Parameters and notations

Symbol	Description	Value
k	index of interfering sector	1, …, 7
R_k	sector radius	92 m
R_k^{in}	inner region radius	75 m
R_{f}	serving region radius	20, 25, …, 40 m
N	total number of RBs in each sub-band	20
s	index of operating sub-band	1, 2, 3
d	distance of the home user to the FAP	5 m
α	outdoor path loss exponent	4
β	indoor path loss exponent	2
w	wall penetration loss	10 dB
$\sigma_{\mathrm{sh}}^{\mathrm{out}}$	outdoor shadowing std	8 dB
$\sigma_{\mathrm{sh}}^{\mathrm{in}}$	indoor shadowing std	6 dB
P_{m}/σ^2	target SNR at the macrocell BS	10
P_{f}/σ^2	target SNR at the FAP	varied
W	femtocell bandwidth	10 MHz
W_{f}	allocated bandwidth of the femtocell user	varied
λ_{h}	bandwidth ratio of a handed over MU	1/40, …, 4/40
N_{h}	number of handed over MUs	varied

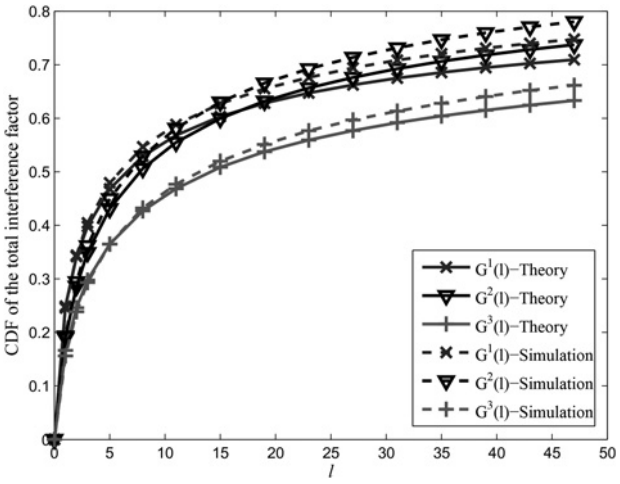

Fig. 5 *CDF of the total interference factor* ***at the FAP C***

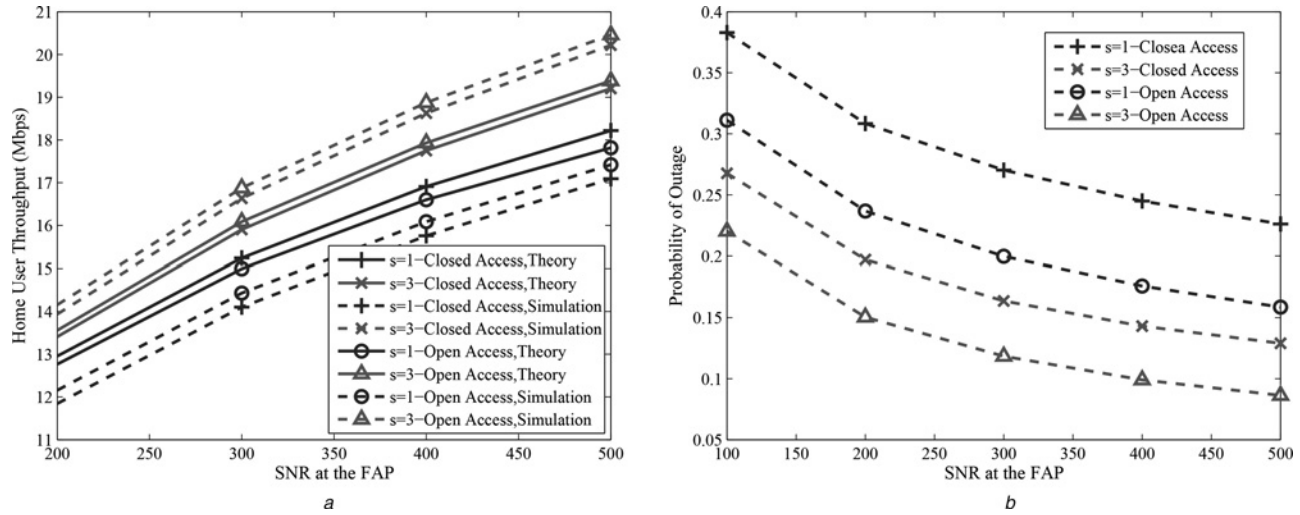

Fig. 6 *Home user throughput and outage probability of the FAP B*

a Throughput
b Probability of outage

the same results obtained through the simulation, that is, the best sub-band.

To study the effect of our power allocation scheme on the macro tier, here, the throughput of the macro tier is evaluated and illustrated in Fig. 7. For the sake of the simplicity and without any loss of the generality, we suppose a simple case in which equal target rate $C_m = 0.5$ bps/Hz is considered for all MUs. It can be shown that the throughput of MUs occupying different RBs of the same sub-band have identical distributions (following the same steps as in the femtocell user calculations). So, we only need to plot the macro tier throughput separately for different sub-bands (the results for $s = 2$ is the same as $s = 3$). From this figure, for the closed access mode the femto tier has insignificant effect on the macro tier because of the effective allocation of the FAP's target power on all sub-bands. However, as expected, with the open access mode, this throughput increases because of the reuse of the bandwidth by handed over MUs.

Finally, we apply our resource allocation scheme for all three FAPs in both closed and open access modes. The results of the resource allocation procedure are given in Table 2 for different values of $P_{\text{out}}^{\max}$ assuming that R_{f} is chosen from the set {20, 25, 30, 35, 40} and λ_{h} is chosen from the set {1/40, 2/40, 3/40, 4/40}. Please note that in all the cases considered here, the convergence of our resource allocation scheme is obtained in less than four iterations. For comparisons, in Table 2, the home user's throughput, best resource allocation, and the outage probability results are given in some cases based on the simulation as well. As stated before, for the FAP A, the open access has no effect on the performance for practical values of R_{f}, and sub-band 1 remains to be the best choice. This result coincides with the result of the method proposed in [13]. We can see that for the less acceptable outage probability, as expected, the home user's required power is increased. Simulation results (which are provided for the case $P_{\text{out}}^{\max} = 0.125$) show that the specified power P_{f} satisfies the outage probability constraint.

For the FAP B, our results show that sub-bands 2 or 3 are the best choice in all examples considered; unlike the method of [13], in which the sub-band 1 is always selected for all FAPs located in the inner region of the sector. Moreover, the previous method do not offer any approach to specify the parameters of an open access FAP. Simulation results show that our method improves the home user's throughput for about 15–35% for different values of R_{f} and λ_{h} compared to the method of [13]. Simulation results provided for both closed and open access modes show good

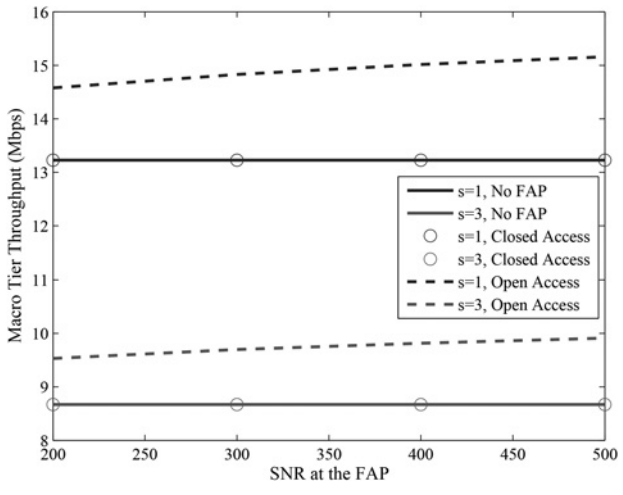

Fig. 7 *Sum throughput of the macro tier on each sub-band*

Table 2 Resource allocation results

FAP	P_{f}/σ^2	T_{f}^{s}	s	R_{f}	λ_{h}	$P_{\text{out}}^{\max}$
A-closed	40.4	8.59	1	—	—	0.25
A-closed	249	20.95	1	—	—	0.125
simulation	249	22.09	1	—	—	0.06
B-closed	174	13.24	2	—	—	0.25
simulation	174	13.09	2	—	—	0.21
B-open	107	10.36	2	25	1/20	0.25
B-open	174	13.19	2	25	1/20	0.22
simulation	174	13.06	2	20	1/20	0.18
C-closed	270	17.57	1	—	—	0.25
simulation	270	17.85	1	—	—	0.19
C-open	95	11.37	1	25	1/20	0.25
C-open	270	18.88	1	35	1/40	0.19
simulation	270	18.8	1	40	1/40	0.11

doi: 10.1049/iet-com.2013.0645

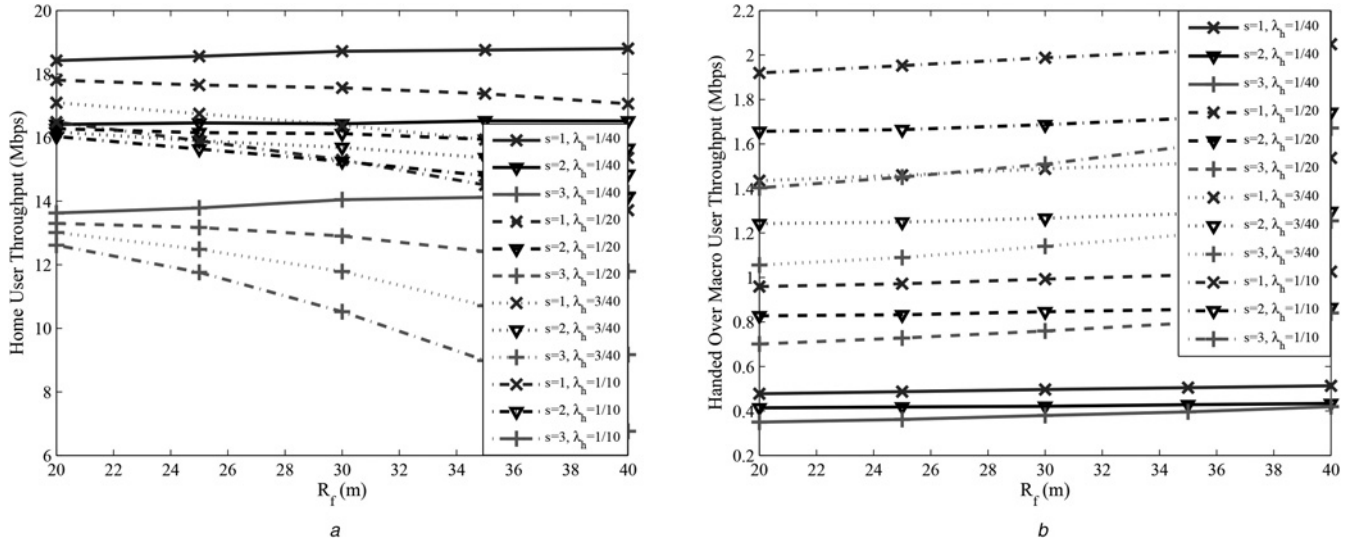

Fig. 8 *Throughput of the home user and handed over MU of the FAP C against R_f*

a Home user throughput
b Handed over MU throughput

compatibility with our analytical analyses except in the value of R_f in the open access mode. However, please note that it has an insignificant effect (about 0.3%) on the throughput of the femtocell user, that is, T_f^s. We can also see that with an effective resource allocation, the open access mode outperforms the closed access mode. For example, for equal P_{out}^{max}, open access mode results in a reduced femtocell required power. In other words, for equal P_f, the outage probability decreases, and the femtocell user's throughput increases in the open access mode.

The advantages of our method can also be observed in the case of the FAP C, which is located in the outer region of the sector. To see the effect of different resource allocation schemes on the performance of the home user, in Fig. 8*a* we have plotted the home user's throughput against the radius of the FAP's serving region for different sub-bands and different λ_hs, considering $P_f/\sigma^2 = 270$. As expected, the sub-band 1 shows the best performance while in [13] one of the sub-bands 2 or 3 is considered for an outer region FAP; which indicates that at least 15% improvement in T_f^s is achieved. We can see that λ_h has a decreasing effect on the home user's throughput, but the effect of R_f is not easily predictable, and its effect in fact changes with P_f, λ_h and the specified sub-band. Fig. 8*b* shows the throughput of a handed over MU, which indicates the effect of the constraint (preserving the MU's performance) on the resource allocation procedure. For example, if MU's throughput more than 500 kbps is required, $\lambda_h = 1/40$ should not be used when considering sub-bands 2 or 3, but it is feasible for sub-band 1 with $R_f = 35$ or 40. In this case, the best resource allocation is sub-band 1 with $R_f = 40$ m and $\lambda_h = 1/40$; which verifies our analytical results except in the value of R_f. However, please note that, it has a very negligible effect (about 0.2%) on the throughput of the home user. We can also see that for an open access FAP, only an effective resource allocation (sub-band, R_f, and λ_h) provides improvements in T_f^s compared to the closed access mode (considering equal powers in both access modes). Here, the home user's throughput in the closed access mode is 17.85, and Fig. 8*a* shows that for the open access mode, the throughput exceeds this value only for some of the resource allocations, and more particularly our method provides the best result.

6 Conclusion

A decentralised static resource allocation scheme using interference statistics for both closed and open access femtocells is presented. The interference statistics derived here can be used as a framework to study different static interference management schemes for two tier femtocell networks. The interference model and the resource allocation method introduced here need to be calculated once based on some simple measurements. The performance of the proposed scheme is evaluated for three femtocells around the reference sector and simulation results show good compatibility with our analyses. It has been observed that with a good sub-band allocation, a femtocell located in a low interference region may prefer closed access mode in order to benefit from both security and higher throughput, for example, FAP A. On the other hand, a femtocell located in the high interference region may prefer to benefit from all interference management methods, such as open access, higher power and choosing the best sub-band, to ensure its good performance, for example, FAP C. Compared to the previous method, our proposed resource allocation scheme shows at least 15% improvement in the throughput of the home user for the cases considered. Although we established our analyses on the assumption of employing SFR in the macro tier, it can be easily extended to other reuse patterns.

7 Acknowledgments

This work is partly sponsored by the Advanced Communication Research Institute (ACRI), Tehran, Iran.

8 References

1 Alouini, M.-S., Goldsmith, A.: 'Area spectral efficiency of cellular mobile radio systems'. IEEE 47th Vehicular Technology Conf., 1997, May 1997, vol. 2, pp. 652–656
2 Chandrasekhar, V., Andrews, J., Gatherer, A.: 'Femtocell networks: a survey', *IEEE Commun. Mag.*, 2008, **46**, (9), pp. 59–67
3 Calin, D., Claussen, H., Uzunalioglu, H.: 'On femto deployment architectures and macrocell offloading benefits in joint macro-femto deployments', *IEEE Commun. Mag.*, 2010, **48**, (1), pp. 26–32

4 Saquib, N., Hossain, E., Le, L.B., Kim, D.I.: 'Interference management in OFDMA femtocell networks: issues and approaches', *IEEE Wirel. Commun.*, 2012, **19**, (3), pp. 86–95
5 Golaup, A., Mustapha, M., Patanapongpibul, L.: 'Femtocell access control strategy in umts and lte', *IEEE Commun. Mag.*, 2009, **47**, (9), pp. 117–123
6 Giuliano, R., Monti, C., Loreti, P.: 'WiMAX fractional frequency reuse for rural environments', *IEEE Wirel. Commun.*, 2008, **15**, (3), pp. 60–65
7 Ali, S., Leung, V.: 'Dynamic frequency allocation in fractional frequency reused ofdma networks', *IEEE Trans. Wirel. Commun.*, 2009, **8**, (8), pp. 4286–4295
8 Mohades, Z., Tabataba Vakili, V., Razavizadeh, S.M., Abbasi-Moghadam, D.: 'Dynamic fractional frequency reuse (dffr) with amc and random access in wimax system', *Wirel. Pers. Commun.*, 2013, **68**, (4), pp. 1871–1881
9 Rahman, M., Yanikomeroglu, H.: 'Enhancing cell-edge performance: a downlink dynamic interference avoidance scheme with inter-cell coordination', *IEEE Trans. Wirel. Commun.*, 2010, **9**, (4), pp. 1414–1425
10 Agustin, A., Vidal, J., Munoz-Medina, O., Fonollosa, J.: 'Decentralized weighted sum rate maximization in mimo-ofdma femtocell networks'. Proc. 2011 IEEE GLOBECOM Workshops (GC Wkshps), December 2011, pp. 270–274
11 Cheung, W.C., Quek, T., Kountouris, M.: 'Throughput optimization, spectrum allocation, and access control in two-tier femtocell networks', *IEEE J. Sel. Areas Commun.*, 2012, **30**, (3), pp. 561–574
12 Oh, D.-C., Lee, H.-C., Lee, Y.-H.: 'Cognitive radio based femtocell resource allocation'. Proc. 2010 Int. Conf. on Information and Communication Technology Convergence (ICTC), November 2010, pp. 274–279
13 Juang, R.-T., Ting, P., Lin, H.-P., Lin, D.-B.: 'Interference management of femtocell in macro-cellular networks'. Wireless Telecommunications Symp. (WTS), 2010, April 2010, pp. 1–4
14 Lee, P., Lee, T., Jeong, J., Shin, J.: 'Interference management in LTE femtocell systems using fractional frequency reuse'. Proc. 12th Int. Conf. on Advanced Communication Technology (ICACT), 2010, February 2010, vol. 2, pp. 1047–1051
15 Lee, T., Yoon, J., Lee, S., Shin, J.: 'Interference management in OFDMA femtocell systems using fractional frequency reuse'. Proc. 2010 Int. Conf. on Communications, Circuits and Systems (ICCCAS), July 2010, pp. 176–180
16 Chowdhury, M., Jang, Y.M., Haas, Z.: 'Interference mitigation using dynamic frequency re-use for dense femtocell network architectures'. Proc. Second Int. Conf. on Ubiquitous and Future Networks (ICUFN), 2010, 2010, pp. 256–261
17 Kim, T.-H., Lee, T.-J.: 'Throughput enhancement of macro and femto networks by frequency reuse and pilot sensing'. IEEE Int. Performance, Computing and Communications Conf., 2008 (IPCCC 2008), December 2008, pp. 390–394
18 Xia, P., Chandrasekhar, V., Andrews, J.: 'Open against closed access femtocells in the uplink', *IEEE Trans. Wirel. Commun.* , 2010, **9**, (12), pp. 3798–3809
19 Stuber, G.L.: 'Principles of mobile communication' (Kluwer Academic Publishers, 2002), pp. 102
20 Salati, A., Nasiri-Kenari, M., Sadeghi, P.: 'Distributed subband, rate and power allocation in OFDMA based two-tier femtocell networks using fractional frequency reuse'. Proc. 2012 IEEE Wireless Communications and Networking Conf. (WCNC), April 2012, pp. 2626–2630
21 Fewell, M.P.: 'Area of common overlap of three circles'. Tech. Rep. DSTO-TN-0722, Defence Science and Technology Organisation, Australia, October 2006
22 Lee, H., Han, K., Hwang, Y., Choi, S.: 'Opportunistic band sharing for point-to-point link connection of cognitive radios'. Proc. Fourth Int. Conf. on Cognitive Radio Oriented Wireless Networks and Communications, 2009 (CROWNCOM '09), June 2009, pp. 1–6

9 Appendix

9.1 Intersection area of two and three circles

Consider two circles A and B with radii r_1 and r_2, and distance d between their centres. The area of their intersection is calculated as [21]

$$S(A \cap B) = r_1^2(\theta - \sin\theta\cos\theta) + r_2^2(\eta - \sin\eta\cos\eta) \tag{21}$$

where $\theta = \arccos\left(f_{\lim}\left((r_1^2 + d^2 - r_2^2)/2r_1 d\right)\right)$, and $\eta = \arccos\left(f_{\lim}\left((r_2^2 + d^2 - r_1^2)/2r_2 d\right)\right)$ where

$$f_{\lim}(x) = \text{sign}(x) + (x - \text{sign}(x))(u(x+1) - u(x-1)) \tag{22}$$

Here, we need to calculate $S(M_k^{\text{in}} \cap I_k^c(l) \cap F)$ and $S(M \cap I_k^c(l) \cap F)$ as the intersection area of three circles. In order to determine $S(M_k^{\text{in}} \cap I_k^c(l) \cap F)$, first we consider some simple situations, that is

$$S(M_k^{\text{in}} \cap I_k^c(l) \cap F) = \begin{cases} 0 & F \cap M_k^{\text{in}} = \emptyset (D_{O_1O_F} \geq R_k^{\text{in}} + R_{\text{f}}) \\ S(I_k^c(l) \cap F) & F \cap M_k^{\text{in}} = F (D_{O_1O_F} \leq R_k^{\text{in}} - R_{\text{f}}) \end{cases} \tag{23}$$

However, the main problem arises when F and M_k^{in} are partly overlapped, that is, $R_k^{\text{in}} - R_{\text{F}} < D_{O_1O_F} < R_k^{\text{in}} + R_{\text{F}}$. In this case, for small enough l and large enough l the problem is simplified to finding the area of the intersection of two circles

$$S(M_k^{\text{in}} \cap I_k^c(l) \cap F) = \begin{cases} S(M_k^{\text{in}} \cap F) & F \subset I_k^c(l) \left(l \leq \left(\frac{D_k}{R_{\text{f}}} - 1\right)^{\alpha}\right) \\ S(M_k^{\text{in}} \cap I_k^c(l)) & I_k^c(l) \subset F \left(l \geq \left(\frac{D_k}{R_{\text{f}}} + 1\right)^{\alpha}\right) \end{cases} \tag{24}$$

Since both O_2 and O_F lie on the x axis in Fig. 2, for F to be a subset of $I_k^{\text{c}}(l)$, we should have $x_c - r \leq D_k - R_{\text{f}}$ and $x_c + r \geq D_k + R_{\text{f}}$ which leads to $l \leq (D_k/R_{\text{f}} - 1)^{\alpha}$. Similarly, for $I_k^{\text{c}}(l)$ to be a subset of F, we should have $l \geq (D_k/R_{\text{f}} + 1)^{\alpha}$.

To achieve an acceptable estimate of $S(M_k^{\text{in}} \cap I_k^{\text{c}}(l) \cap F)$ for $(D_k/R_{\text{f}} - 1)^{\alpha} < l < (D_k/R_{\text{f}} + 1)^{\alpha}$, it is notable to know that for these values of l, $S(M_k^{\text{in}} \cap I_k^{\text{c}}(l) \cap F)$ decreases with the increase of l, that is, $I_k^{\text{c}}(l)$ becomes smaller and covers less parts of the region F with the increase of l. Thus, we consider a linear extrapolation between its two extreme values, that is, a decreasing line between $S(M_k^{\text{in}} \cap F)$ and $S\left(M_k^{\text{in}} \cap I_k^{\text{c}}\left((D_k/R_{\text{f}} + 1)^{\alpha}\right)\right)$. The approximate value should also be less than $S(M_k^{\text{in}} \cap I_k^{\text{c}}(l))$. Thus, we approximate $S(M_k^{\text{in}} \cap I_k^{\text{c}}(l) \cap F)$ by

$$\min\left(S(M_k^{\text{in}} \cap I_k^{\text{c}}(l)), S(M_k^{\text{in}} \cap F) - \left[S(M_k^{\text{in}} \cap F) - S\left(M_k^{\text{in}} \cap I_k^{\text{c}}\left(\left(\frac{D_k}{R_{\text{f}}} + 1\right)^{\alpha}\right)\right)\right] \times \left(l^{(1/\alpha)} - \frac{D_k}{R_{\text{f}}} + 1\right)/2\right)$$

For $S(M \cap I_k^{\text{c}}(l) \cap F)$, we can take same procedures to make an appropriate approximation.

doi: 10.1049/iet-com.2013.0645